Role of Microtubules in Osteogenic Differentiation of Mesenchymal Stem Cells on 3D Nanofibrous Scaffolds

Sai Rama Krishna Meka,[†,‡] Leeba Ann Chacko,[†,§,⊥] Ashwini Ravi,[§] Kaushik Chatterjee,[‡,§] and Vaishnavi Ananthanarayanan*,[§]

‡Department of Materials Engineering and §Centre for BioSystems Science and Engineering, Indian Institute of Science, Bangalore 560012, India

S *Supporting Information*

ABSTRACT: Human bone marrow mesenchymal stem cells (MSCs) cultured on three-dimensional (3D) nanofibrous scaffolds are known to undergo osteogenic differentiation even in the absence of soluble osteoinductive factors. Although this process of differentiation has been attributed to the shape that cells assume on the fibrous scaffolds, it is unclear how constriction of cell shape would contribute to the differentiation phenotype. Here, we quantitatively compared cell and nuclear morphologies of cells cultured on 3D poly(ε-caprolactone) (PCL) nanofibers (NF) and two-dimensional (2D) flat films using confocal fluorescence microscopy. We discovered that while cells on the 2D films exhibited cellular and nuclear morphologies similar to those cultured on tissue culture polystyrene, cells cultured on the 3D NF showed distinct cell and nuclear morphologies, with lower areas and perimeters, but higher aspect ratios. We next tested the effect of treatment of cells with actin-depolymerizing cytochalasin D and microtubule-depolymerizing nocodazole on these morphologies. In both 2D and 3D scaffolds, actin depolymerization brought about gross changes in cell and nuclear morphologies. Remarkably, microtubule depolymerization resulted in a phenotype similar to actin depolymerization in cells cultured on 3D NF alone, indicating a significant role for the microtubule cytoskeleton in the maintenance of cell shape and structure in 3D. The morphological changes of the nucleus that were apparent upon cytoskeletal perturbation were reflected in the organization of heterochromatin in the nucleus, with MSCs on 3D alone exhibiting a differentiation phenotype. Finally, we tested the effect of cytoskeletal depolymerization on mineralization of cells. Again, we observed higher mineralization in cells cultured on 3D NF, which was lost in cells treated with either cytochalasin D or nocodazole. Taken together, our results suggest that both the actin and microtubule cytoskeletons contribute significantly toward maintenance of cell and nuclear shape in cells cultured on 3D scaffolds, and consequently to their osteogenic differentiation.

KEYWORDS: *cytoskeleton, stem cells, osteogenesis, nanofibers, tissue scaffolds*
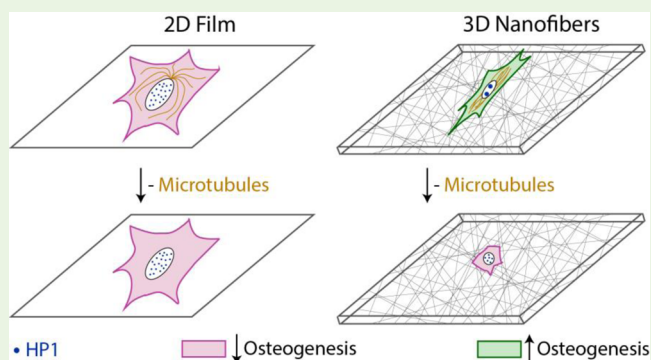
INTRODUCTION

Adult mesenchymal stem cells (MSCs) that are derived from the bone marrow are capable of differentiating into different cell types such as osteoblasts, myoblasts, chondrocytes, neurons, and stromal cells.[1] The use of MSCs in the treatment of human diseases has become an important part of therapeutic medicine[2] and this use stems from their intrinsic property of being multipotent,[1] as well as their ability to egress and migrate away from their niche.[3] For several decades, MSCs in vitro have been made to differentiate into specific cell lineages with the aid of epigenetic modifications, the use of growth factors, cytokines, corticosteroids and hormones.[4] However, these conventional methods of in vitro differentiation of MSCs tend to be expensive and are often suboptimal in generating a desired mature phenotype with good efficiency.

In recent years, it was discovered that growing MSCs on artificially made substrates of varying stiffness can also drive their differentiation into specific cell types over time.[5,6] Several groups have reported that culture of stem cells on soft substrates leads to their differentiation into soft tissue such as the brain tissue, whereas growing these cells on hard substrates leads to their differentiation into hard tissue such as osteogenic tissue.[7,8] These substrates of varying stiffness correspond to the stiffness of the extra cellular matrix (ECM) of different native tissues inside the body and helps guide stem cell differentiation into distinct tissue lineages.

Culturing stem cells on substrates of different architectures or topographies also elicits varying responses, with MSCs grown on a fibrous three-dimensional (3D) substrate behaving and differentiating differently than when grown on a flat two-dimensional (2D) substrate.[9−12] Several studies have also shown that merely differing the material used to make these

microenvironments and changing the architecture of these 3D scaffolds can elicit varying differentiation and behavioral patterns of MSCs, without the use of extrinsic factors.[13−17] All of these studies indicate that MSCs are able to perceive their microenvironment and differentiate in response to cues from that environment.

Therefore, it is important to understand how MSCs interact with their external environment, transduce information about their environs and ultimately undergo gene expression changes in order to differentiate into a specific cell lineage. The primary mechano-sensing element in the cell is the cytoskeleton, which communicates with the ECM. Specifically, cells grown on different environments have differential expression of focal adhesion proteins and actin cytoskeletal network.[18−20] In addition, perturbing the actin cytoskeleton and its associated motor, nonmuscle myosin II, hinders the differentiation process of MSCs when grown on these different substrates.[8,21,22] However, less is known about what role the microtubules play in this differentiation process in a 3D environment. In this study, we aim to understand the role of the microtubule cytoskeleton in the differentiation of MSCs to osteoblasts when grown on 3D nanofibrous scaffolds.

■ METHODS

Preparation and Characterization of 2D Films and 3D Nanofibrous Scaffolds. 12% w/v of polymer solution was prepared by dissolving PCL (Mn ∼ 80 000, Sigma) in trifluoroethanol (Sigma) and kept for stirring overnight. The 2D thin films were prepared by spin coating technique (spinNXG-P1). Five hundred microliters of PCL solution was spin-coated on the aluminum sheet (5 cm × 5 cm) at 5000 rpm for 40 s to obtain thin films of uniform thickness. The 3D NF scaffolds were prepared by electrospinning (Espin Nano, India). The PCL solution fed through 2 mL syringe at 0.5 mL/h was electrospun by applying a voltage of 12 kV for 1 h with the collector placed at 12 cm from the spinneret to obtain dense fibrous mats with uniform nanofiber diameter. The prepared thin films and NF were gold-coated to examine their morphology under SEM (FEI, Germany).

Cell Culture. Primary human bone marrow-derived MSCs (Poietics, Lonza, USA) from a 22-year old male donor were cultured in growth medium (MSC Basal Medium Lonza) supplemented with SingleQuot (gentamicin + amphotericin, FBS and L-glutamine, MSC Growth Medium, Lonza). Thin films and electrospun NF scaffolds were cut into circular discs (10 mm diameter) to fit in the wells of 48 well plates. Prior to cell seeding, the scaffolds were sterilized under UV for 1 h. One ×10^4 cells were seeded per sample with 0.4 mL culture medium and medium was refreshed every 3 days. To assess the ability of the nanofibers to induce stem cell osteogenesis in the absence of soluble factors, cells were cultured on 2D films in the absence and presence of soluble ostoegenic factors, as detailed in the Supporting Information.

Cytochalasin D and Nocodazole Treatments. The role of actin and microtubules in MSC fate when cultured on 2D and 3D surfaces was studied using their inhibitors, cytochalasin D (CytoD, Sigma) and nocodazole (Noc, Sigma), respectively. The inhibitors were initially dissolved in DMSO and various working concentration of Noc (50 nM, 500 nM and 1 μM) and CytoD (1 μM) were prepared in growth media. The specific concentration of drugs used is mentioned in the figure captions. For quantification of the cell and nuclear parameters in inhibitor-treated cells, phalloidin-actin staining and DAPI staining were employed (see below).

Antibody Staining. To visualize the actin and microtubule cytoskeleton or to examine the effect of inhibitors on cell and nuclear morphology, samples at day 4 and 14 were fixed in 3.7% formaldehyde for 15 min, permeabilized with 0.2% TritonX-100 for 5 min and blocked in 2.5% BSA for 30 min. Subsequently, samples were incubated in phalloidin-Alexa Fluor 546 or 488/1:100 rabbit anti-α-

tubulin primary and 1:1000 antirabbit Alexa Fluor 488 secondary (Thermoscientific) for 15 min, followed by DAPI (Thermoscientific) for 1 min to stain F-actin/microtubule and nuclei, respectively. Samples were imaged using a confocal microscope (INCell Analyzer 6000, GE). Samples were washed in PBS in every intermittent step and the dyes were prepared in 2.5% BSA. Further, the effect of inhibitors on nuclear organization was examined through studying their heterochromatin. Samples at day 4 and 14 were fixed in 3.7% formaldehyde for 15 min, permeabilized with 0.2% TritonX-100 for 5 min and incubated in 2.5% BSA for blocking for 30 min. The washed samples were incubated at 4 °C overnight in antihuman heterochromatin protein 1 α-subunit (HP1α) primary antibody raised in rabbit (Thermoscientific) prepared at 1:100 dilution in 2.5% BSA. The samples were washed thoroughly in PBS followed by incubation in Alexa 488 conjugated antirabbit secondary antibody raised in mouse (Thermoscientific) at 1:1000 dilution for 2 h at room temperature. Washed samples were imaged using a confocal microscope.

Mineralization. In vitro mineralization on scaffolds was studied at day 14 by staining the fixed scaffolds with 2% Alizarin red S dye (Sigma) for 30 min. The samples were washed thoroughly with deionized water to remove the unbound dye. The samples were visually assessed by collecting the images of stained scaffolds. Further mineral quantification was done spectroscopically at 405 nm after extracting the calcium bound alizarin red dye by incubating the samples in 5% SDS and 0.5 N HCL for 30 min. The data is presented through plotting the absorbance values. Mineral deposits at day 21 (see Supporting Information) were imaged in SEM and quantified through EDAX.

Microscopy, Image Processing, and Analysis. Imaging of fluorescently stained MSCs grown on 2D films and 3D NF in 48-well plates was carried out on an INCell Analyzer 6000 (GE Healthcare), with 10× 0.45 NA, 40× 0.60 NA, or 60× 0.70 NA air objectives, fitted with an sCMOS 5.5 Mp camera, with an x−y pixel separation of 650, 160, and 108 nm, respectively. The fixed samples were hydrated in PBS while imaging. For all images, Z-stacks with 15−21 steps and step size 1 μm, encompassing the entire cell was acquired. Maximum intensity projection of the Z-stack was performed for the analysis of cell and nuclear shape and size parameters. Fiji/ImageJ Software was employed for obtaining the maximum intensity projection of the Z-stacks and for analysis of HP1 foci in the nucleus.

For counting the number of HP1 foci, maximum intensity projections of Z-stacks of the HP1 stained nuclei were first background corrected. The projections were then subjected to intensity thresholding to retain 1−2% of the maximum pixel intensities to identify the foci. Diameter of the foci was obtained by drawing circular ROIs around the foci and using the "Measure" function in Fiji/ImageJ.

All data were analyzed and plots were generated using Matlab. Statistical analyses were performed in Matlab using one-way or two-way ANOVA followed by Tukey-Kramer posthoc test for significance.

■ RESULTS

1. 3D Electrospun Nanofibers Have a Diameter of ∼600 nm. The surface topography of PCL thin films examined through SEM (Figure 1, left) was found to be homogeneously smooth. Further, SEM image of electrospun fibers (Figure 1, right) confirmed the 3D nanofibrous architecture with uniform fiber diameter of 600 ± 50 nm (mean ± s.d., n = 10 fibers from 3 independent samples). We then tested the attachment and growth of MSCs on 3D NF and the potential of these cells to undergo osteogenic differentiation in the absence of osteogenic supplements (Figures S1−S3). Consistent with previous findings,[16,17] we observed that MSCs cultured on 3D NF devoid of osteogenic supplements for 14 or 21 days exhibited osteogenic profiles similar to that of cells grown on 2D films supplemented with osteogenic factors.

2. Cytoskeleton of Cells on 3D NF Appears Compact. To compare the cytoskeletal morphology of cells cultured on 2D films and 3D NF, phalloidin and anti-α-tubulin antibody-
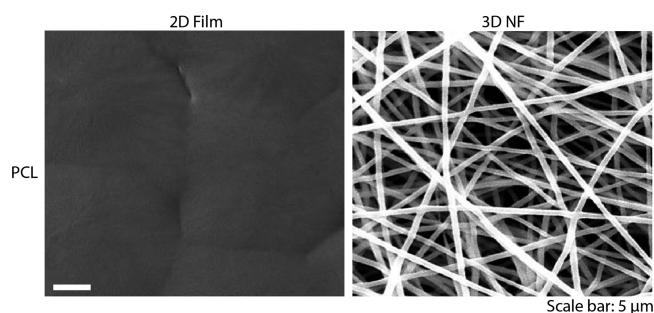
Figure 1. Representative SEM images of spin coated 2D PCL film (left) and electrospun 3D NF (right).

stained cells were imaged using confocal microscopy (Figure 2). Strikingly, cells on 3D NF (Figure 2A, B, bottom, green) were visibly smaller and narrower than cells on 2D films (Figure 2A, B, top, green), which resembled cells conventionally grown on tissue culture polystyrene (TCPS). Similarly, the nuclei of cells on 3D NF (Figure 2A, B, bottom, blue) appeared smaller than those on 2D films (Figure 2A, B, top, blue).

Additionally, the actin and microtubule cytoskeleton appeared more compact, and less discernible as single bundles in cells grown on 3D NF (Figure 2A, B, bottom, green). The radial microtubule arrangement that was apparent on cells cultured on 2D films (Figure 2B, top, green) was not visible in cells on 3D NF (Figure 2B, bottom, green). In fact, in cells cultured on 3D NF, the arrangement of the actin and the microtubule cytoskeleton appeared identical.

3. Depolymerization of the Microtubule Cytoskeleton of Cells Grown on 3D NF Disrupts Their Cellular and Nuclear Morphology. The actin cytoskeleton has been implicated to be important for differentiation of MSCs grown on TCPS.[21,23] Because both the actin and microtubule cytoskeletons appear modified in cells grown on 3D NF, we sought to evaluate the role of the microtubule cytoskeleton in a 3D nanofibrous environment. MSCs were thus cultured on 2D films and 3D NF in DMSO (control) and different concentrations of Noc. The change in cellular and nuclear morphologies in these cells was visualized by fluorescent phalloidin and DAPI staining followed by confocal microscopy (Figure 3). In cells on 2D films, there was very little difference in the morphology of the cell and the nucleus when treated
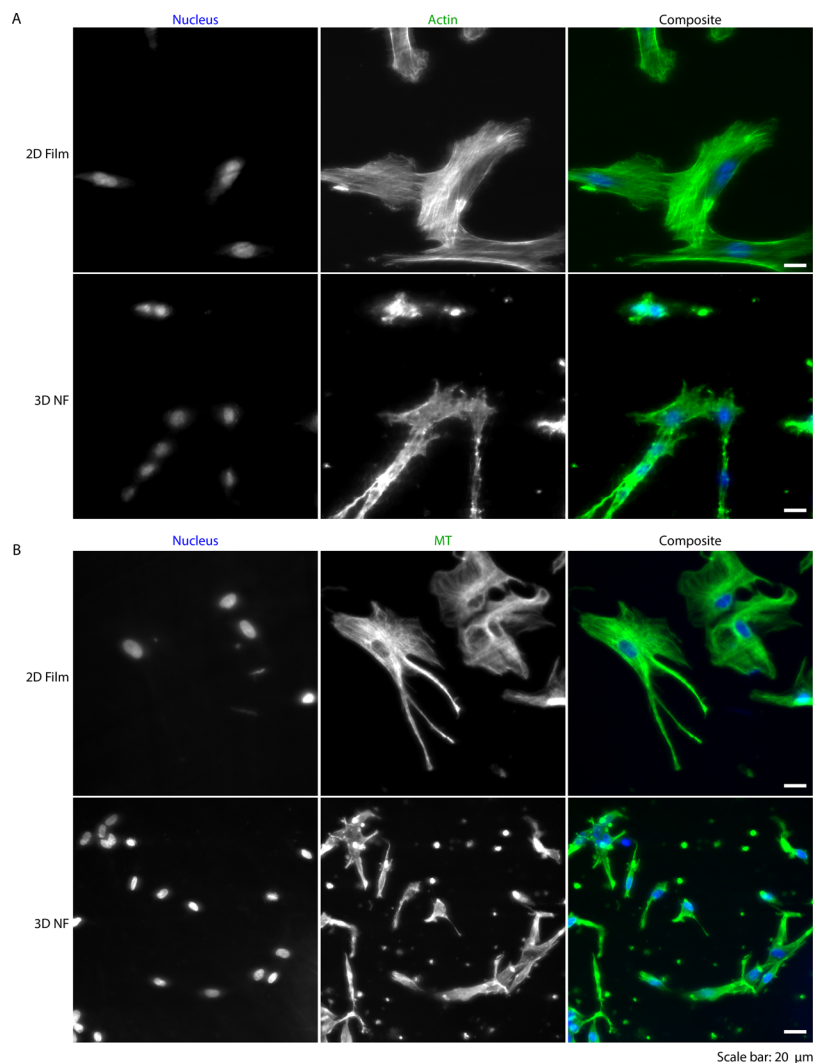

Figure 2. (A) Representative confocal images of the actin (green) and nuclei (blue) of cells cultured for 4 days on 2D films (top) and 3D NF (bottom). (B) Confocal images showing the microtubules (green) and nuclei (blue) of cells cultured for 4 days on 2D films (top) and 3D NF (bottom).
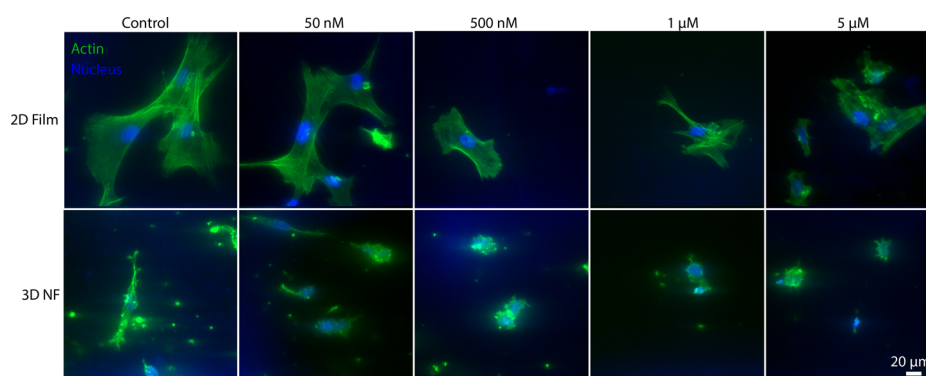
Figure 3. Representative confocal images of actin (green) and nuclei (blue) of cells grown on 2D film (top) and 3D NF (bottom) for 4 days in the absence ("DMSO") and presence of increasing concentrations of Noc ("50 nM", "500 nM", "1 μM," and "5 μM").
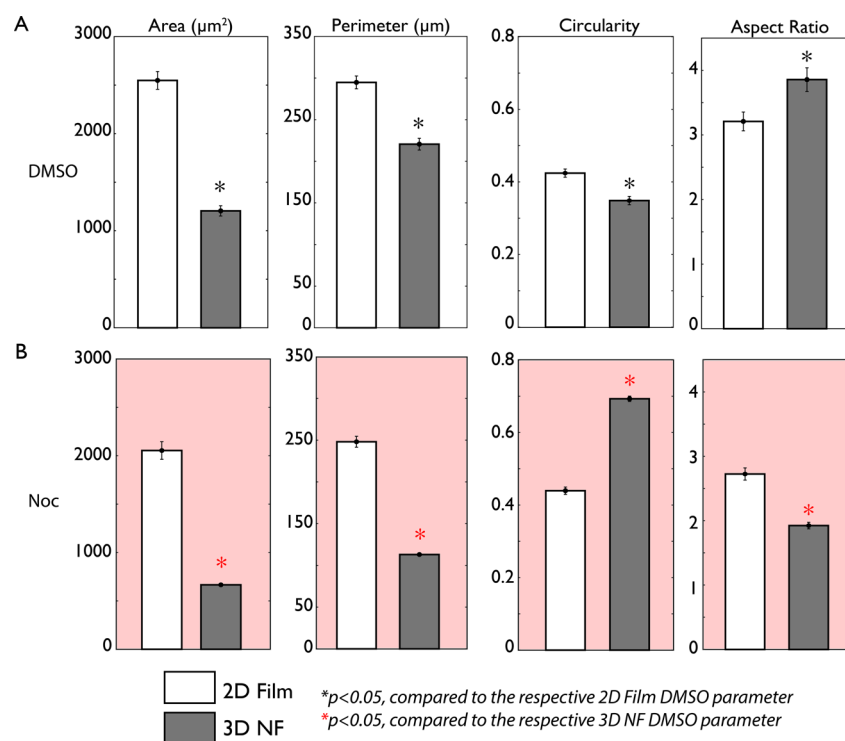

Figure 4. Quantification of cell morphology parameters viz. area, perimeter, circularity, and aspect ratios in cells cultured for 4 days on 2D films (white bars) and 3D NF (gray bars) (A) in DMSO control and (B) in the presence of 500 nM Noc, stained with phalloidin-Alexa Fluor 488 ($n >$ 160 cells in all cases). Note that for cells cultured on 2D, only the area and perimeter showed statistically significant difference ($p < 0.05$) between DMSO control and Noc treated cells. Error bars represent the standard error of the mean (s.e.m).

with progressively increasing concentrations of Noc (Figure 3, top). However, in cells cultured on 3D NF, changes in the cellular and nuclear morphologies were visible starting with a concentration of 500 nM (Figure 3, bottom).

4. Both Actin and Microtubule Cytoskeletons Are Required to Maintain Cellular and Nuclear Shape in 3D. To quantify the changes in the cell and nuclear morphologies upon treatment with CytoD and Noc, images of fluorescent phalloidin- and DAPI-stained cells were analyzed using Fiji/ImageJ. The area, perimeter, circularity and aspect ratio measurements were obtained using Fiji's in-built "Measure" function after drawing a region of interest around individual cells. As observed before, cells on 2D films were ~2.5× larger and more spread out as evidenced by their area and perimeter than those on 3D (Figure 4, top).

Treatment of cells on 3D NF with minimal concentration of 500 nM Noc reduced their area by ~4× and perimeter by ~2×, while at the same time increasing their circularity to 0.7 and reducing the aspect ratio to 2, as compared to those on DMSO (Figure 4, bottom). In contrast, MSCs cultured on both 2D films and 3D NF showed a drastic difference in their cell shape and size parameters when treated with 1 μM CytoD (Figure S4).

The nuclei of cells on 3D NF again exhibited smaller area and perimeter as compared to cells on 2D film (Figure 5, top). While treatment of cells on 2D film with CytoD alone caused a change in nuclear morphology (Figure 5, middle, white bars), treatment of cells on 3D NF with minimal concentration of either CytoD (1 μM) or Noc (500 nM) affected the nuclear morphology, with a significant decrease in area, perimeter and aspect ratio (Figure 5, gray bars, middle and bottom).
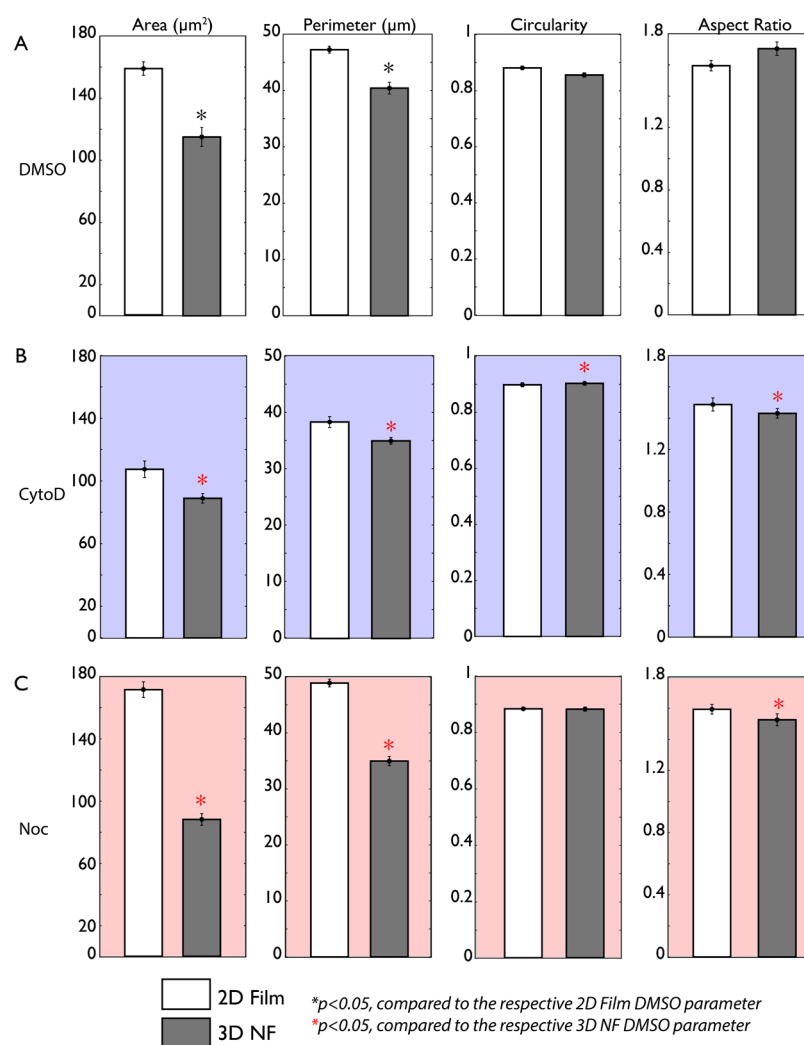
Figure 5. Quantification of nuclear morphology parameters viz. area, perimeter, circularity and aspect ratios in cells cultured for 4 days on 2D films (white bars) and 3D NF (gray bars) in DMSO control (A), in the presence of 1 μm CytoD (B) and 500 nM Noc (C) stained with DAPI ($n > 50$ nuclei in all cases). Error bars represent s.e.m. Note that for cells cultured on 2D, there was no statistical difference between the nuclear parameters of DMSO control and Noc treated cells whereas the area and perimeter of CytoD treated cells were statistically different ($p < 0.05$) from the DMSO control.

5. Organization of Heterochromatin in Cells on 3D NF is Perturbed by Treatment with Cytoskeletal Inhibitors.

We observed that MSCs devoid of the actin or the microtubule cytoskeleton on 3D NF exhibited altered cellular and nuclear morphologies. Altered nuclear morphologies have been observed to alter the organization of heterochromatin in the nucleus and hence, the expression of genes.[24] In particular, undifferentiated stem cells have been shown to exhibit small spots of heterochromatin spread throughout the cell, as observed by staining the heterochromatin protein HP1.[25]

So, we set out to test if the altered nuclear and cellular morphology of cells on 3D in the presence of cytoskeletal depolymerizing drugs had an effect on the HP1 staining in the nuclei of these cells. For cells cultured on 2D films, in control cells as well as cells treated with minimal concentrations of CytoD and Noc, HP1 staining showed ~25 small foci of HP1 per nucleus. In addition, these foci had a diameter of 0.6 ± 0.1 μm ($n = 20$ spots from 10 nuclei) and were homogeneously distributed across the nucleus, indicative of a "stem-like", undifferentiated state (Figure 6A, top and 6B, left). In 3D NF however, control cells treated with DMSO exhibit a drastically

different heterochromatin organization, with only around 10 foci per nucleus that are twice as large (1.1 ± 0.2 μm, $p < 0.0001$, $n = 20$ spots from 10 nuclei) as the HP1 foci in the nuclei of cells grown on 2D films, indicative of a more differentiated state (Figure 6A, bottom, white arrowheads and Figure 6B, right). This organization of HP1 disappears in MSCs cultured on 3D NF that were treated with CytoD or Noc (Figure 6A, bottom, and Figure 6B, right, "CytoD" and "Noc"), indicating a role for both the actin and microtubule cytoskeletons in the differentiation of MSCs cultured on 3D NF.

6. Disruption of the Cytoskeleton Reduces the Osteogenic Differentiation of cells Cultured on 3D NF.

To directly test the role of the actin and microtubule cytoskeleton on differentiation of MSCs cultured on 3D NF to osteoblasts, the mineralization of cells was tested using alizarin red staining on 14-day cultures grown in the absence (DMSO) and presence of cytoskeletal inhibitors (CytoD and Noc). We observed that the mineralization that was observed in untreated cells was almost halved in both CytoD and Noc treated cells (Figure 7), indicating the participation of both
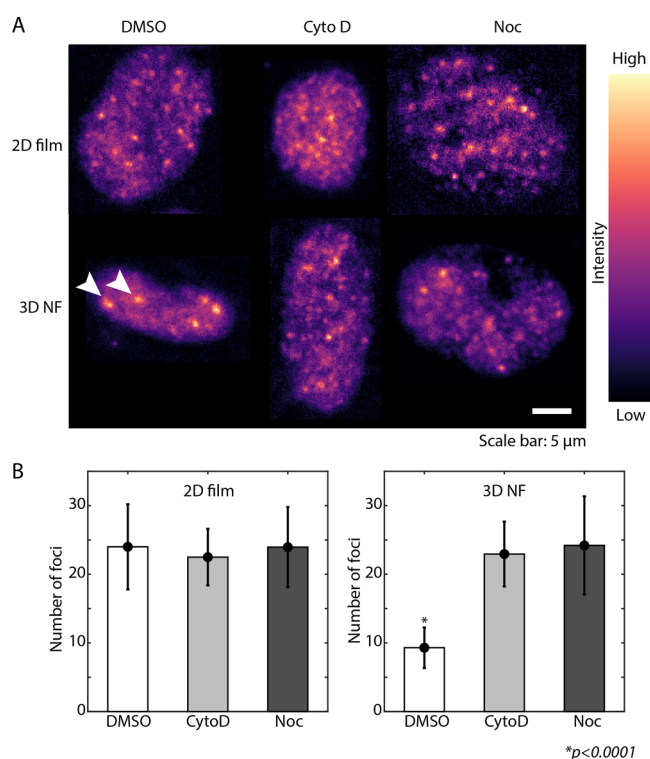
Figure 6. (A) Intensity map of organization of HP1 in nuclei of MSCs cultured for 14 days in the presence of DMSO, CytoD and Noc in 2D (top) and 3D (bottom) environment ($n > 80$ nuclei in all cases). Only the nuclei of cells cultured on 3D NF in DMSO exhibit distinct, large foci (white arrowheads). (B) Quantification of the number of HP1 foci in the nuclei of cells cultured on 2D film (left, $n = 20$ nuclei for each case) and 3D NF (right, $n = 20$ nuclei for each case) in the absence ("DMSO") and presence of cytoskeletal inhibitors ("CytoD" and "Noc"). Error bars represent the standard deviation.

filaments in the process of osteogenic differentiation of MSCs on 3D fibrous scaffolds.

DISCUSSION

Differences in Cellular and Nuclear Morphology between MSCs Cultured on 2D and 3D. Nanofibrous scaffolds have emerged as a popular class of tissue scaffolds in recent years owing to the similarity in the architecture of the scaffold to that the fibrous architecture of the natural extracellular matrix (ECM). Moreover, MSCs cultured on these nanofibrous scaffolds have also been shown to undergo osteogenic differentiation in the absence of osteogenic factors in the culture medium.[16,17] Here too, we observed this property of 3D NF to initiate osteogenic pathways of differentiation of MSCs.

We observed that MSCs grown on 3D NF have a much smaller area and perimeter, but higher aspect ratio. The nuclei of these cells are also smaller and less rounded than those grown in the 2D scaffolds. In the 2D scaffolds, MSCs are likely able to spread out due to the continuous underlying layer of substrate. However, in the case of the cells growing in the 3D scaffolds, the cells assume a smaller area because of the constraints imposed by the arrangement of the fibrous scaffolds. Previous studies have shown that restricting the area of cell spreading affects the cytoskeleton structure, which in turn affects the nuclear morphology and dynamics.[24,26,27] Although MSCs cultured on 3D NF do not migrate deep into the 3D
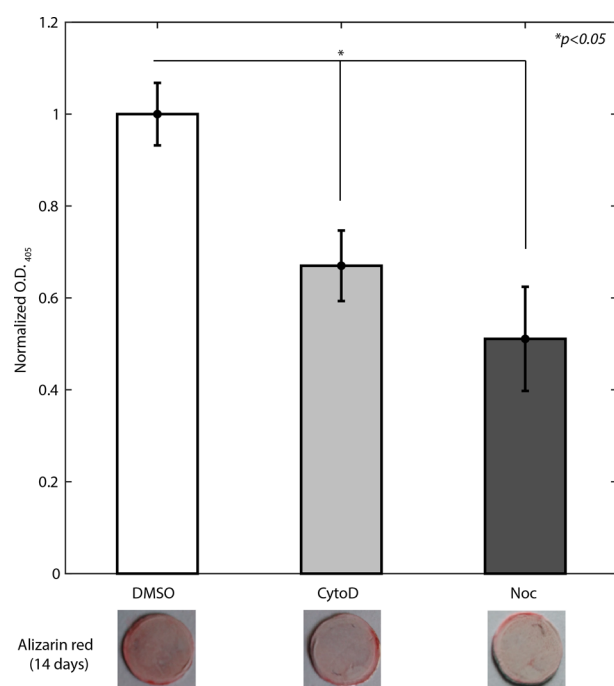

Figure 7. Plot of the mineralization of MSCs treated with DMSO (control), CytoD, and Noc normalized to the control DMSO value cultured on 3D NF for 14 days without osteogenic supplements ($n = 3$ replicates). The images of the alizarin red staining are displayed below the respective plot. Error bars represent the standard deviation.

mesh,[16] there seems to be constraint on the cell spreading due to the nanofibrous nature of the substrate. This restriction of spread of cells on NF could also affect the cell matrix adhesions that form in the 3D environment.[28] Increasing the pore size in 3D NF by incorporation of gelatin[29] has been demonstrated to improve migration of MSCs into PCL 3D NF. It would be interesting to study the effect of this increased pore size and migration in the context of cell spreading and the accompanying cytoskeletal changes.

Reorganization of Actin and Microtubule Cytoskeleton in 3D NF. The cell tensegrity model proposes a balance between the forces of the tension-bearing actin and compression-resistant microtubules.[30,31] A change in these forces by cytoskeletal disruption or modification of adhesion of cells to the substrate has been demonstrated to lead to changes in cell shape, growth, proliferation, and as a result, cell adhesion and fate.[32−35] The drastic rearrangement of the actin and microtubule cytoskeleton MSCs cultured on 3D NF could result in a new force balance between the tensile and compressive forces, leading to changes in the shape of the cell and the nucleus that we observed. This in turn, could be one of the factors modulating the differentiation of MSCs on 3D NF.

Remodeling of the actin cytoskeleton is a common feature of stem cells that undergo differentiation, with the accompanying cell shape and cytoskeletal tension changes modulating the fate of these cells.[8,36] Thus far, the microtubule cytoskeleton has not been considered to play a definitive role, because unlike actin, which undergoes considerable remodeling upon differentiation, the characteristic radial arrangement of microtubules is retained during the differentiation of MSCs.[37] During differentiation of keratinocytes to epithelial cells, the microtubule cytoskeleton is known to undergo a drastic reorganization from radial bundles

to cortical arrays.[38] Here too, we observe a change in the organization of the cytoskeleton of MSCs cultures on 3D NF; both actin and microtubules appear more compactly located within the cell, but more strikingly, microtubules no longer appear to be radially arranged.

Effect of Cytoskeletal Perturbations on Cells Growing in 2D and 3D Environments. We demonstrated that disrupting the actin cytoskeleton affects cellular and nuclear morphology in both 2D films and 3D NF. This result is consistent with previous reports.[26] Surprisingly, however, only MSCs growing in the 3D NF environment were affected by Noc treatment. Also this change in cellular morphology due to Noc treatment is dose-dependent, with changes in morphology being observed at concentrations of 500 nM and above. Hence, the microtubules seem to play a vital role in maintaining the integrity of the cells in the 3D environment, suggesting that cells and their nuclei in 3D environment are more sensitive to perturbations of the microtubule cytoskeleton.

For cells grown in 2D, it has been demonstrated that the actin cytoskeleton pulls on the nucleus on its sides and the stress fibers push the nucleus down, thus flattening the nucleus. Conversely, microtubules push against the nucleus with a force opposing that of actin. Thus, disrupting actin and microtubules affects the size and shape of the nucleus.[26,39] Interestingly, in our experiments, we observed that for MSCs grown on 3D NF, disruption of the actin or the microtubule cytoskeleton reduces the area of the nucleus as well as the aspect ratio.

While the disruption of the microtubule cytoskeleton in differentiated adherent cells has been demonstrated to increase cellular adhesion and contractility[35] via the RhoA activator GEF-H1 without an apparent change in cell area,[40] for the MSCs we cultured on 3D NF, Noc treatment does not elicit the same response. Future experiments will help delineate the role of the microtubule in its function in cell contractility in 2D vs 3D.

Differentiation of MSCs in the 3D Environment and the Role of Microtubules in the Differentiation Process. In stem cells, the DNA is normally loosely packed with large regions of euchromatin, with most of the genes being expressed; in differentiated cells, however, there are relatively fewer regions of euchromatin, with several genes being turned off. Thus, differentiated cells contain more regions of heterochromatin.[25] We visualized these regions of heterochromatin by staining for the heterochromatin protein HP1. Only the MSCs grown in the 3D environment showed distinct, large HP1 punctae while cells on 2D exhibited smaller and diffuse HP1 spots. This suggests that MSCs growing on 3D NF were undergoing differentiation. Perturbation of either the actin or the microtubule cytoskeleton affected the formation of these HP1 punctae indicating that both the cytoskeletal elements participate in the process of differentiation in 3D.

Further, we observed stronger alizarin red staining in 3D NF than in 2D indicating enhanced osteogenesis in MSCs grown in the 3D environment. Also, perturbing either the actin cytoskeleton or the microtubules halves the production of calcium deposits in the 3D NF, as can be seen with the reduction in alizarin red staining. This strengthens our observation that both the actin and the microtubule filaments are essential for differentiation of MSCs to osteoblasts on 3D NF. This observation is unique to MSCs on 3D NF, because MSCs on 2D rely primarily on the actin cytoskeleton to dictate their osteogenic cell fate when grown in the presence of supplements.[41,42] In the former, focal adhesion complexes comprising integrins as the primary sensor, serve as a communication link between the ECM and the actin cytoskeleton.[43] Future work will help uncover how microtubules might sense the ECM in MSCs that undergo osteogenic differentiation on 3D NF.

CONCLUSION

We demonstrate that the cytoskeleton plays differential roles in cells cultured on 2D films than those on 3D fibrous scaffolds. The form assumed by the cytoskeleton of cells on 3D NF is likely a result of constraints on cell spreading. This restriction in turn translates to altered cellular and nuclear morphology, with a concomitant change in the organization of heterochromatin in the nucleus. This in turn likely affects the gene expression profile of MSCs on 3D NF. Both the actin and microtubule cytoskeletal filaments participate in the differentiation process of MSCs in the 3D environment, with perturbation of either affecting the organization of heterochromatin and hence, the mineralization that accompanies osteogenic differentiation of MSCs.

ASSOCIATED CONTENT

⑤ Supporting Information

The Supporting Information is available free of charge on the ACS Publications website at DOI: 10.1021/acsbiomaterials.6b00725.

SI Materials and Methods, SI Results, Figures S1−S4 (PDF)

AUTHOR INFORMATION

Corresponding Author
*E-mail: vaish@be.iisc.ernet.in.

ORCID ⓘ
Vaishnavi Ananthanarayanan: 0000-0003-2936-7853

Present Address
⊥L.A.C. is currently at Mechanobiology Institute, National University of Singapore, Singapore

Author Contributions
†S.R.K.M and L.A.C. contributed equally to this report

Notes
The authors declare no competing financial interest.

REFERENCES

(1) Trounson, A.; McDonald, C.; Abbott, A.; Aboody, K. S.; Brown, A.; Rainov, N. G.; Bower, K. A.; Liu, S.; Yang, W.; Small, J. E.; et al. Stem Cell Therapies in Clinical Trials: Progress and Challenges. *Cell Stem Cell* **2015**, *17* (1), 11−22.

(2) Trounson, A.; DeWitt, N. D. Pluripotent stem cells progressing to the clinic. *Nat. Rev. Mol. Cell Biol.* **2016**, *17* (3), 194−200.

(3) Katayama, Y.; Battista, M.; Kao, W.-M.; Hidalgo, A.; Peired, A. J.; Thomas, S. A.; Frenette, P. S. Signals from the sympathetic nervous system regulate hematopoietic stem cell egress from bone marrow. *Cell* **2006**, *124* (2), 407−421.

(4) Snykers, S.; De Kock, J.; Rogiers, V.; Vanhaecke, T. In vitro differentiation of embryonic and adult stem cells into hepatocytes: state of the art. *Stem Cells* **2009**, *27* (3), 577–605.

(5) Cozzolino, A. M.; Noce, V.; Battistelli, C.; Marchetti, A.; Grassi, G.; Cicchini, C.; Tripodi, M.; Amicone, L.; Cozzolino, A. M.; Noce, V.; et al. Modulating the Substrate Stiffness to Manipulate Differentiation of Resident Liver Stem Cells and to Improve the Differentiation State of Hepatocytes. *Stem Cells Int.* **2016**, *2016*, 1–12.

(6) Park, J. S.; Chu, J. S.; Tsou, A. D.; Diop, R.; Tang, Z.; Wang, A.; Li, S. The effect of matrix stiffness on the differentiation of mesenchymal stem cells in response to TGF-β. *Biomaterials* **2011**, *32* (16), 3921–3930.

(7) Engler, A. J.; Griffin, M. A.; Sen, S.; Bönnemann, C. G.; Sweeney, H. L.; Discher, D. E. Myotubes differentiate optimally on substrates with tissue-like stiffness: pathological implications for soft or stiff microenvironments. *J. Cell Biol.* **2004**, *166* (6), 877–887.

(8) Engler, A. J.; Sen, S.; Sweeney, H. L.; Discher, D. E. Matrix elasticity directs stem cell lineage specification. *Cell* **2006**, *126* (4), 677–689.

(9) Hildebrandt, C.; Büth, H.; Cho, S.; Impidjati; Thielecke, H. Detection of the osteogenic differentiation of mesenchymal stem cells in 2D and 3D cultures by electrochemical impedance spectroscopy. *J. Biotechnol.* **2010**, *148* (1), 83–90.

(10) Shekaran, A.; Sim, E.; Tan, K. Y.; Chan, J. K. Y.; Choolani, M.; Reuveny, S.; Oh, S.; Tolar, J.; Blanc, K.; Keating, A.; et al. Enhanced in vitro osteogenic differentiation of human fetal MSCs attached to 3D microcarriers versus harvested from 2D monolayers. *BMC Biotechnol.* **2015**, *15* (1), 102.

(11) Tian, X.-F.; Heng, B.-C.; Ge, Z.; Lu, K.; Rufaihah, A. J.; Fan, V. T.-W.; Yeo, J.-F.; Cao, T. Comparison of osteogenesis of human embryonic stem cells within 2D and 3D culture systems. *Scand. J. Clin. Lab. Invest.* **2008**, *68* (1), 58–67.

(12) Tutak, W.; Jyotsnendu, G.; Bajcsy, P.; Simon, C. G. Nanofiber scaffolds influence organelle structure and function in bone marrow stromal cells. *J. Biomed. Mater. Res., Part B* **2016**.

(13) Jahani, H.; Kaviani, S.; Hassanpour-Ezatti, M.; Soleimani, M.; Kaviani, Z.; Zonoubi, Z. The effect of aligned and random electrospun fibrous scaffolds on rat mesenchymal stem cell proliferation. *Cell J.* **2012**, *14* (1), 31–38.

(14) Prabhakaran, M. P.; Venugopal, J. R.; Ramakrishna, S. Mesenchymal stem cell differentiation to neuronal cells on electrospun nanofibrous substrates for nerve tissue engineering. *Biomaterials* **2009**, *30* (28), 4996–5003.

(15) Villa-Diaz, L. G.; Brown, S. E.; Liu, Y.; Ross, A. M.; Lahann, J.; Parent, J. M.; Krebsbach, P. H. Derivation of mesenchymal stem cells from human induced pluripotent stem cells cultured on synthetic substrates. *Stem Cells* **2012**, *30* (6), 1174–1181.

(16) Kumar, G.; Tison, C. K.; Chatterjee, K.; Pine, P. S.; McDaniel, J. H.; Salit, M. L.; Young, M. F.; Simon, C. G. The determination of stem cell fate by 3D scaffold structures through the control of cell shape. *Biomaterials* **2011**, *32* (35), 9188–9196.

(17) Meka, S. R. K.; Jain, S.; Chatterjee, K. Strontium eluting nanofibers augment stem cell osteogenesis for bone tissue regeneration. *Colloids Surf., B* **2016**, *146*, 649–656.

(18) Ryoo, S.-R.; Kim, Y.-K.; Kim, M.-H.; Min, D.-H. Behaviors of NIH-3T3 fibroblasts on graphene/carbon nanotubes: proliferation, focal adhesion, and gene transfection studies. *ACS Nano* **2010**, *4* (11), 6587–6598.

(19) Bu, S.-C.; Kuijer, R.; van der Worp, R. J.; van Putten, S. M.; Wouters, O.; Li, X.-R.; Hooymans, J. M. M.; Los, L. I. Substrate Elastic Modulus Regulates the Morphology, Focal Adhesions, and α-Smooth Muscle Actin Expression of Retinal Müller Cells. *Invest. Ophthalmol. Visual Sci.* **2015**, *56* (10), 5974–5982.

(20) Yeung, T.; Georges, P. C.; Flanagan, L. A.; Marg, B.; Ortiz, M.; Funaki, M.; Zahir, N.; Ming, W.; Weaver, V.; Janmey, P. A. Effects of substrate stiffness on cell morphology, cytoskeletal structure, and adhesion. *Cell Motil. Cytoskeleton* **2005**, *60* (1), 24–34.

(21) Müller, P.; Langenbach, A.; Kaminski, A.; Rychly, J. Modulating the actin cytoskeleton affects mechanically induced signal transduction and differentiation in mesenchymal stem cells. *PLoS One* **2013**, *8* (7), e71283.

(22) Sonowal, H.; Kumar, A.; Bhattacharyya, J.; Gogoi, P.; Jaganathan, B.; Bruder, S.; Fink, D.; Caplan, A.; Ito, H.; Krane, S.; et al. Inhibition of actin polymerization decreases osteogeneic differentiation of mesenchymal stem cells through p38 MAPK pathway. *J. Biomed. Sci.* **2013**, *20* (1), 71.

(23) Yourek, G.; Hussain, M. A.; Mao, J. J. Cytoskeletal changes of mesenchymal stem cells during differentiation. *ASAIO J.* **2007**, *53* (2), 219–228.

(24) Li, Q.; Kumar, A.; Makhija, E.; Shivashankar, G. V. The regulation of dynamic mechanical coupling between actin cytoskeleton and nucleus by matrix geometry. *Biomaterials* **2014**, *35* (3), 961–969.

(25) Mattout, A.; Aaronson, Y.; Sailaja, B. S.; Raghu Ram, E. V.; Harikumar, A.; Mallm, J.-P.; Sim, K. H.; Nissim-Rafinia, M.; Supper, E.; Singh, P. B.; et al. Heterochromatin Protein 1 β (HP1β) has distinct functions and distinct nuclear distribution in pluripotent versus differentiated cells. *Genome Biol.* **2015**, *16*, 213.

(26) Ramdas, N. M.; Shivashankar, G. V. Cytoskeletal Control of Nuclear Morphology and Chromatin Organization. *J. Mol. Biol.* **2015**, *427* (3), 695–706.

(27) McNamara, L. E.; Burchmore, R.; Riehle, M. O.; Herzyk, P.; Biggs, M. J. P.; Wilkinson, C. D. W.; Curtis, A. S. G.; Dalby, M. J. The role of microtopography in cellular mechanotransduction. *Biomaterials* **2012**, *33* (10), 2835–2847.

(28) Baker, B. M.; Chen, C. S. Deconstructing the third dimension: how 3D culture microenvironments alter cellular cues. *J. Cell Sci.* **2012**, *125* (13), 3015–3024.

(29) Binulal, N. S.; Natarajan, A.; Menon, D.; Bhaskaran, V. K.; Mony, U.; Nair, S. V. Gelatin nanoparticles loaded poly(ε-caprolactone) nanofibrous semi-synthetic scaffolds for bone tissue engineering. *Biomed. Mater.* **2012**, *7* (6), 065001.

(30) Ingber, D. E. Cellular tensegrity: defining new rules of biological design that govern the cytoskeleton. *J. Cell Sci.* **1993**, *104*, 613–627.

(31) Chen, C. S.; Ingber, D. E. Tensegrity and mechanoregulation: from skeleton to cytoskeleton. *Osteoarthr. Cartil. Osteoarthr. Res. Soc.* **1999**, *7*, 81–94.

(32) Chen, C. S.; Mrksich, M.; Huang, S.; Whitesides, G. M.; Ingber, D. E. Geometric Control of Cell Life and Death. *Science* **1997**, *276* (5317), 1425.

(33) Chen, C. S.; Alonso, J. L.; Ostuni, E.; Whitesides, G. M.; Ingber, D. E. Cell shape provides global control of focal adhesion assembly. *Biochem. Biophys. Res. Commun.* **2003**, *307* (2), 355–361.

(34) Coyer, S. R.; Singh, A.; Dumbauld, D. W.; Calderwood, D. A.; Craig, S. W.; Delamarche, E.; García, A. J. Nanopatterning reveals an ECM area threshold for focal adhesion assembly and force transmission that is regulated by integrin activation and cytoskeleton tension. *J. Cell Sci.* **2012**, *125* (21), 5110–5123.

(35) Elineni, K. K.; Gallant, N. D. Microtubules Mechanically Regulate Cell Adhesion Strengthening Via Cell Shape. *Cell. Mol. Bioeng.* **2014**, *7* (1), 136–144.

(36) McBeath, R.; Pirone, D. M.; Nelson, C. M.; Bhadriraju, K.; Chen, C. S. Cell shape, cytoskeletal tension, and RhoA regulate stem cell lineage commitment. *Dev. Cell* **2004**, *6* (4), 483–495.

(37) Rodríguez, J. P.; González, M.; Ríos, S.; Cambiazo, V. Cytoskeletal organization of human mesenchymal stem cells (MSC) changes during their osteogenic differentiation. *J. Cell. Biochem.* **2004**, *93*, 721–731.

(38) Lechler, T.; Fuchs, E. Desmoplakin: an unexpected regulator of microtubule organization in the epidermis. *J. Cell Biol.* **2007**, *176* (2), 147–154.

(39) Makhija, E.; Jokhun, D. S.; Shivashankar, G. V. Nuclear deformability and telomere dynamics are regulated by cell geometric constraints. *Proc. Natl. Acad. Sci. U. S. A.* **2016**, *113* (1), E32–40.

(40) Chang, Y.-C.; Nalbant, P.; Birkenfeld, J.; Chang, Z.-F.; Bokoch, G. M. GEF-H1 couples nocodazole-induced microtubule disassembly to cell contractility via RhoA. *Mol. Biol. Cell* **2008**, *19* (5), 2147–2153.

(41) Mathieu, P. S.; Loboa, E. G. Cytoskeletal and focal adhesion influences on mesenchymal stem cell shape, mechanical properties,

and differentiation down osteogenic, adipogenic, and chondrogenic pathways. *Tissue Eng., Part B* **2012**, *18* (6), 436−444.

(42) Titushkin, I.; Cho, M. Modulation of Cellular Mechanics during Osteogenic Differentiation of Human Mesenchymal Stem Cells. *Biophys. J.* **2007**, *93* (10), 3693−3702.

(43) Hynes, R. O. Integrins: versatility, modulation, and signaling in cell adhesion. *Cell* **1992**, *69* (1), 11−25.